Commonwealth Edison
One First National Plaza, Chicago, Illinois
Address Reply to: Post Office Box 767
Chicago, Illinois 60690

August 10, 1981

Mr. Dennis M. Crutchfield, Chief
Operating Reactors Branch 5
U.S. Nuclear Regulatory Commission
Washington, DC 20555

Subject: Dresden Station Units 2 and 3
Seismic Analysis for Installation
of Five and Ten High Density Fuel
Storage Racks
NRC Docket Nos. 50-237/249

Reference (a): "Licensing Report Dresden Nuclear
Power Plant Units 2 and 3
Spent Fuel Rack Modification",
Rev. 5, dated 1-19-81.

Dear Mr. Crutchfield:

Enclosed for your review are the results of the seismic analyses performed for the installation of five and ten new high density spent fuel storage racks of the type described in Reference (a).

These analyses were performed using the conservative assumptions discussed in the conference call between Commonwealth Edison Company, Quadrex Corp., and the NRC staff on July 24, 1981.

As discussed previously, interim installation of five or ten new fuel storage racks in the Dresden 3 fuel pool will preclude the need to transfer fuel in fuel shipping casks from the Dresden 3 fuel pool to the Dresden 2 fuel pool in order to support the January 1982 Dresden 3 refueling outage. The fuel transfers would be necessary to maintain the ability to unload the core to facilitate NRC required modifications to the feedwater spargers. The five or ten new racks will provide the additional spaces necessary to accomplish core unloading without fuel transfers.

Please address any questions concerning this matter to this office.

A026
s/l

One (1) signed original and thirty-nine (39) copies of this transmittal are provided for your use.

Very truly yours,

T J Rausch

T. J. Rausch
Nuclear Licensing Administrator
Boiling Water Reactors

cc: Region III Inspector, Dresden
Mr. John Wolfe, Esq.
Dr. Linda W. Little
Dr. Forest J. Renwick
Ms. Mary Jo Murray

lm

2389N

Dresden Nuclear Station

Evaluation of Spent Fuel Pool and Racks for Five and Ten Racks Impacting on Pool Floor

1.0 INTRODUCTION

It has been proposed that existing spent fuel racks at the north end of the Dresden 3 pool be replaced with 5 or 10 new high-density fuel racks. The scope of the present evaluation is to determine whether the spent fuel pool floor and walls can withstand the additional loads resulting from rocking of the racks during a postulated safe shutdown earthquake. In the absence of nonlinear rocking and sliding analysis for the loaded rack, the magnitude of the maximum uplift was computed earlier using an energy-balance method based on the maximum sliding velocity of an empty rack. This uplift value was computed to be 0.76 inch. However, for the present evaluation to be conservative, this uplift value was arbitrarily increased to 1.0 inch. The existing racks are bolted to the floor, hence, no uplift of these racks was considered.

2.0 ANALYSIS AND EVALUATION OF POOL SLAB

An energy-balance method of analysis was used for evaluating the loads on the pool floor. To determine an upperbound of this load, it was assumed that the entire energy resulting from impact will be absorbed by the strain energy of the pool floor and the impacting rack in a single impact. In other words, the energy that would be left in the rack which would cause it to rebound and rock was not subtracted to compute the energy that needs to be absorbed in the pool floor.

2.1 Input Kinetic Energy

For 1-inch uplift, the angular velocity of the rack was computed to be 0.177 radian per sec. This was determined by equating the restoring moment of the tilted rack to the product of its moment of inertia and angular acceleration and solving the equation of motion. This method of computing the angular velocity, outlined in Reference 1, uses the rack geometry, mass and the uplift value and assumes realistically that the rack behaves as a rigid body while dropping from the tilted position. The vertical impact velocity at the uplifted end of the rack, computed from this angular velocity, was 10.02 in/sec. The velocity of different parts would vary between this maximum value and zero (at the pivoting end). The kinetic energy of impact was calculated using linear velocity distribution. This method of characterizing the motion of a tilted structure has been experimentally verified in Reference 2 and is considered a more accurate representation of the actual phenomena as compared to the alternate method described in the next paragraph. This method is designated as Method I.

An alternative method (Method II) of computing the kinetic energy was also investigated. In this alternative method, the rack was idealized as a beam having a length equal to the width of the rack. The depth of the beam was ignored. The tip of the beam was assumed to be uplifted by 1.0 inch and allowed to be dropped. The velocity of the rack at the uplifted end was computed assuming a free-fall, i.e., velocity equal to $\sqrt{2gh}$ where g is acceleration due to gravity and h is the drop height (i.e., 1.0 inch). Using the uplifted-end velocity (27.8 in/sec.) and a linear velocity distribution, the impact energy was computed by integrating over the length of the idealized beam. The peak velocity computed this way assumed a free drop and is not an accurate representation since the rack does not fall freely, rather rotates pivoting about the other leg. Thus, the phenomenon assumed in this Method II analysis is not considered a true representation of the actual situation, even though, for the purpose of comparison, the pool structures have been evaluated using the input kinetic energy values obtained by both methods.

2.2 Energy Absorbing Characteristics of the Pool Slab

Impact energy is dissipated in the pool slab in three ways:

a) Inertia of the pool slab to movement
b) Strain energy resulting from the local compression of the concrete underneath the rack legs
c) Strain energy resulting from the overall behavior of the floor slab acting as a plate

Since the weight of the supporting pool floor target mass is relatively high, some of the applied energy will be absorbed because of the inertia of the member to movement. The target mass was assumed to be equal to the mass of that portion of concrete pool slab which is contained in the volume bounded by 45-degree inclined planes from the edge of the rack leg and the bottom surface of the pool slab (Reference 3) as shown in Figure 2-1. For computing the maximum rack load and the concrete bearing stress, energy absorption due to inertia of the target mass was not considered.

Strain energy resulting from the local compression of the concrete underneath the rack leg was computed assuming a nonlinear distribution of compressive stress under the rack leg as shown in Figure 2-2. The compressive stress at the interface is equal to the bearing stress and, at the bottom surface, this stress is zero. The variation of this stress across the depth was assumed to be parabolic in computing the equivalent linear spring to represent the local energy absorbing characteristics of the slab.

Strain energy resulting from the overall behavior of the floor slab acting as a plate would depend upon the location of the impact. For the five-rack impact, two such locations were considered:

a) Location A, corresponding to rack legs close to the north wall of the pool, and

b) Location B, corresponding to rack legs away from the wall.

Location A is only 9 inches from the wall. Hence, it was assumed that the energy dissipation resulting from the overall plate-type behavior of the floor would be small and negligible when the rack legs impact in Location A. Location B is about 5.5 ft. from the wall. Energy absorption characteristics for impact at this location were represented by a linear spring, properties of which were computed from the bending behavior of the slab. The moment of inertia of the slab cross-section was computed using the formula in ASCE Standard Manual 58 (Reference 4). This formula provided a moment of inertia larger than that obtained from ACI-318-77 code (Reference 5) (corresponding to actual moment resulting from a floor load which produces shear equal to the shear capacity of the slab). Thus, the use of this formula is considered conservative.

For the ten rack case, the racks impact along two parallel lines: Legs nearest the north wall and legs farthest from the north wall (two parallel rows of 5 racks each). The analysis utilized the same methodology described above and the results reported in Table 2-2a are for impact of the legs nearest the wall which generates the highest load at the support and at a distance, d, from the support.

2.3 Energy Absorbing Characteristics of the Rack

When the racks impact on the pool floor, a part of the impact energy will be absorbed in the form of strain energy of the rack. This energy absorption characteristic was represented by a linear spring constant. This linear spring constant was derived using the vertical stiffness and deflection characteristics of the detailed finite element model of the rack which was originally used for dead load stress analysis.

2.4 Analysis Results and Evaluation of Pool Slab

Using the energy balance method described above, the rack impact load on the pool floor was computed. The computed dynamic amplification factors are listed in Table 2-1. Combining the rack impact load with the dead loads and hydrostatic loads and vertical seismic loads, and assuming very conservatively that all the racks impact simultaneously, the shear load in the pool slab was computed and compared with the allowable values. These are listed in Tables 2-2 and 2-2a, for five and ten racks, respectively. Shear loads were computed at the floor support location (Location A) as well as at a distance d (equal to depth of the slab) from the support (Location B). Comparison of the computed shear loads with the allowable values shows that the pool slab can adequately withstand the total loads, including the impact loads resulting from 1-inch uplift of the loaded racks.

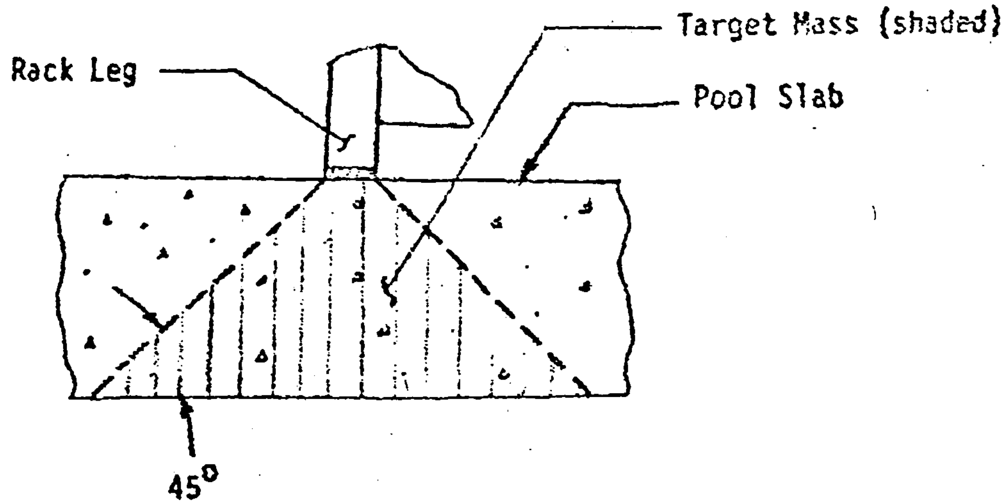

FIGURE 2-1 TARGET MASS UNDER RACK LEG

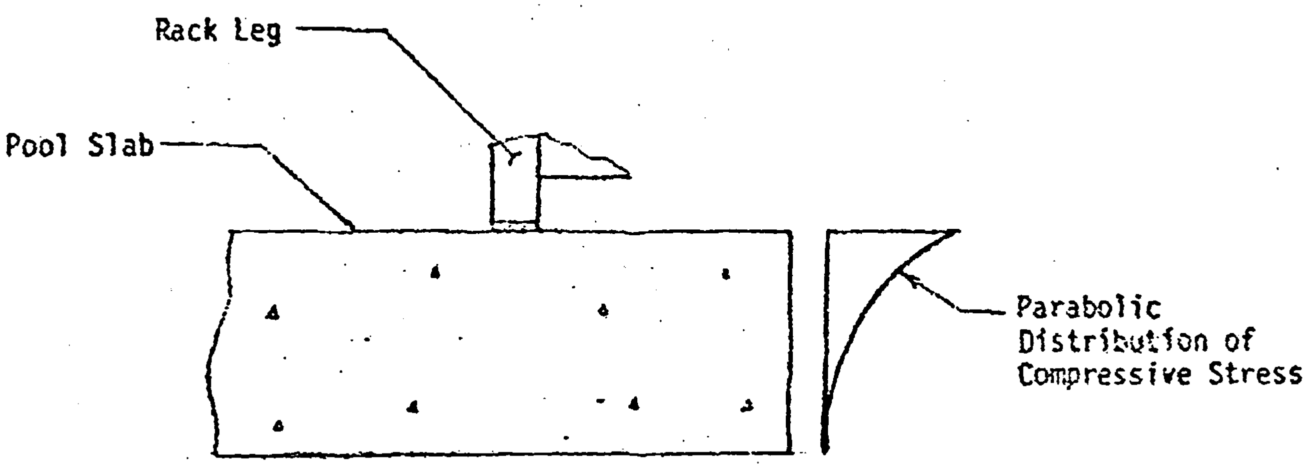

FIGURE 2-2 ASSUMED DISTRIBUTION OF COMPRESSIVE STRESS UNDER RACK LEG

TABLE 2-1

DYNAMIC AMPLIFICATION FACTORS[1]
RESULTING FROM RACK IMPACT

	Location of Drop	
	A	B
Method I	6.5	6.1
Method II	18.1	17.1

NOTE[1]: Dynamic Amplification factor is defined as the ratio of rack leg force during rack impact to the rack leg force due to buoyant weight of the rack applied as a static load.

TABLE 2-2

POOL SLAB ANALYSIS RESULTS FOR FIVE-RACK IMPACT

Estimated Upperbound Uplift = 0.76 in.
Assumed Uplift = 1.0 in.
Maximum Impact Velocity--
Method I : Based on Angular Velocity = 10.02 in/sec
Method II: Based on Free Fall = 27.8 in/sec (See Note 4 below)

Equivalent Uniform Dead Load Without Impact--
5 New Racks + Old Racks = $0.86 K/ft^2$

Total (including seismic) = $4.99 K/ft^2$

Location of Drop	Shear Load (Kip/ft) Using Method I(1)			
	At Support		At Distance d From Support	
	Computed	Allowable	Computed	Allowable
A	65.5	522.2(2)	<40.1	82.6(3)
B	<65.5	522.2(2)	<40.1	82.6(3)

NOTES: (1) Average shear load at the north end of the pool floor

(2) Based on Section 11.7.3 of Reference 5 (Shear Friction)

(3) Based on Section 11.3.1.1 of Reference 5 (i.e., the short formula)

(4) Computed for the purpose of comparison only

TABLE 2-2 (continued)

POOL SLAB ANALYSIS RESULTS FOR
FIVE-RACK IMPACT

Location of Drop	Shear Load (Kip/ft) Using Method II(4)(1)			
	At Support		At Distance d From Support	
	Computed	Allowable	Computed	Allowable
A	129.0	522.2(2)	<40.1	82.6(3)
B	<129.0	522.2(2)	40.1	82.6(3)

NOTES: (1) Average shear load at the north end of the pool floor

(2) Based on Section 11.7.3 of Reference 5 (Shear Friction)

(3) Based on Section 11.3.1.1 of Reference 5 (i.e., the short formula)

(4) Computed for the purpose of comparison only

Table 2-2a

Pool Slab Analysis Results for
Ten-Rack Impact

Equivalent Uniform Dead Load Without Impact--
10 New Racks + Old Racks = 0.98 k/ft^2
Total (including seismic) = 5.13 k/ft^2

Method	Shear Load (kip/ft)(1)			
	At Support		At Distance d From Support	
	Computed	Allowable	Computed	Allowable
Method I	84.1	522.2(2)	52.5	82.6(4)
Method(3) II	179.2	522.2(2)	87.2	85.1(5) 90.8(6)

NOTES:
(1) Average shear load at north end of the pool floor.
(2) Based on Section 11.7.3 of Reference 5 (shear friction)
(3) Computed for the purpose of comparison only.
(4) Based on Section 11.3.1.1 of Reference 5.
(5) Based on Section 11.3.2.1 of Reference 5.
(6) Based on Section 11.3.2.1 of Reference 5 with f'_c increased by 15% due to aging.

3.0 EVALUATION OF RACK STRESSES

Table 3-1 presents the maximum loads on rack legs when the impact force resulting from 1-inch uplift is considered. These are based on impact at Location A, which gives the most critical rack loads. Also, the effect of energy dissipation in target mass inertia was ignored to maximize these rack loads, and no overall pool slab flexibility was considered. Table 3-1 also presents the rack loads from the original fixed-base analysis for the purpose of comparison. Table 3-2 lists the stresses in various critical components of the racks when the effect of impact resulting from 1-inch uplift is included. Comparison of these stresses with the allowable stresses shows that the rack design is adequate and no overstress condition is expected.

TABLE 3-1

MAXIMUM RACK LEG FORCES DUE TO RACK IMPACT ON POOL SLAB

Consideration	Maximum Force (kips)			
	Method I		Method II (1)	
	Corner Leg	Middle Leg	Corner Leg	Middle Leg
Considering Rack Impact Near Wall	92.3	115.4	256.2	320.2
Original Fixed-Base Analysis	179.8	208.9	179.8	208.9

Note: (1) Computed for the purpose of comparison only.

TABLE 3-2

STRESS IN RACK COMPONENTS DUE TO RACK IMPACT ON POOL SLAB (3)

Rack Component	Load Combination	Critical Stress Type	Allowable Stress (ksi) (2)	Computed Stress (ksi)	
				Method I	Method II (1)
Tube Wall	D+B+E'	Membrane	33.5	11.53	31.98
Fuel Support Plate	D+B+E'	Membrane	33.5	9.28	25.74
Filler Plate	D+B+E'	Membrane	33.5	9.19	25.49
Base Grid	D+B+E'	Membrane	33.5	1.70	4.70
Rack Leg	D+B+E'	Membrane	33.5	8.55	23.71
Interface	D+B+E'	Bearing	4.76	0.87	2.42

Note: (1) Computed for the purpose of comparison only.

(2) Using a Dynamic Increase Factor of 1.2 per Reference 4.

(3) Deceleration loads resulting from impact are maximum at the uplifted end (i.e., the impacted end) and zero at the pivoted end. The rack leg reaction forces shown in Table 3-1 are for the impacted legs, and so are based on maximum deceleration values. Thus, the ratio between these reaction forces to the dead load reaction forces gives the conservative scaling factor with which the dead load stresses (from original finite element analysis) were multiplied to obtain the stresses in the rack for impact loads shown in this table.

4.0 EVALUATION OF NORTH WALL

Because of its proximity to the impacting racks, the north wall of the pool will have loads higher than the other walls. This wall was evaluated for the combined load (SSE load case) including the effect of five new racks impacting on the pool floor. Table 4-1 presents the comparison of the shear capacity with the computed shear loads based on impact at the critical Location A, for the five rack case. Table 4-la presents the comparison of the shear capacity with the computed shear loads based on impact of the legs nearest the North wall, which is limiting, for the ten rack case. Results presented in Tables 4-1 and 4-la show that the computed values are well within the shear capacity of the wall for both the five and ten rack cases.

TABLE 4-1

EVALUATION OF THE VERTICAL SHEAR CAPACITY OF THE NORTH WALL (3)

Load Combination	Vertical Shear (kips)		
	Allowable	Computed	
		Method I	Method II[1]
D+L+H+E'+Impact	15,724[2]	3814	4607

Note: (1) Computed for the purpose of comparison only.

(2) Considering the effect of vertical reinforcement in resisting diagonal tension resulting from shear.

(3) Based on the critical impact Location A.

Table 4-1a

EVALUATION OF THE VERTICAL SHEAR CAPACITY OF THE NORTH WALL (3)

Load Combination	Vertical Shear (kips)		
	Allowable	Computed	
		Method 1	Method II (1)
D+L+H+E'+Impact	13,600 (2)	4,270	5,811

Note: (1) Computed for the purpose of comparison only.

(2) Considering the effect of vertical reinforcement in resisting diagonal tension resulting from shear.

(3) Based on impact of legs nearest North wall.

5.0 REFERENCES

1. Housner, G. W., "The Behavior of Inverted Pendulum Structures during Earthquakes," Bulletin of Seisnological Society of America, Vol. 53, No. 2, February, 1963.

2. Aslam, M., Godden, W. G., and Scalise, "Earthquake Rocking Response of Rigid Bodies," J. of Structural Division, ASCE, February, 1980.

3. Topical Report, "Design of Structures for Missile Impact," BC-TOP-9A, Revision 2, Bechtel Power Corporation, 1974.

4. ASCE Manual and Report on Engineering Practice No. 58, "Structural Analysis and Design of Nuclear Plant Facilities," 1980.

5. "Building Code Requirements for Reinforced Concrete," ACI-318-77, American Concrete Institute, 1977.